

ORIGINAL ARTICLE

Obesity Biology and Integrated Physiology



Lower abdominal adipose tissue cannabinoid type 1 receptor availability in young men with overweight

Laura Pekkarinen^{1,2} | Tatu Kantonen^{1,3} | Vesa Oikonen¹ |
 Merja Haaparanta-Solin^{1,4} | Richard Aarnio¹ | Alex M. Dickens^{5,6} |
 Annie von Eyken^{5,6} | Aino Latva-Rasku¹ | Prince Dadson¹ |
 Anna K. Kirjavainen¹ | Johan Rajander⁷ | Kari Kalliokoski¹ |
 Tapani Rönnemaa^{2,8} | Lauri Nummenmaa^{1,9} | Pirjo Nuutila^{1,2}

¹Turku PET Centre, University of Turku, Turku, Finland

²Department of Endocrinology, Turku University Hospital, Turku, Finland

³Clinical Neurosciences, Turku University Hospital, Turku, Finland

⁴MediCity Research Laboratory, University of Turku, Turku, Finland

⁵Turku Bioscience Centre, University of Turku, Turku, Finland

⁶Åbo Akademi University, Turku, Finland

⁷Turku PET Centre, Åbo Akademi University, Turku, Finland

⁸Department of Medicine, University of Turku, Turku, Finland

⁹Department of Psychology, University of Turku, Turku, Finland

Correspondence

Pirjo Nuutila, Turku PET Centre, University of Turku, and Department of Endocrinology, Turku University Hospital, Turku, Finland.
 Email: pirjo.nuutila@utu.fi

Funding information

Academy of Finland, Grant/Award Numbers: 294897, 307402, 332225; Diabetestutkimussäätiö; Emil Aaltosen Säätiö; Jenny ja Antti Wihurin Rahasto; Orionin Tutkimussäätiö; Turun Yliopistollisen Keskussairaalan Koulutus- ja Tutkimussäätiö; Varsinais-Suomen Rahasto

Abstract

Objective: Cannabinoid type 1 receptors (CB1R) modulate feeding behavior and energy homeostasis, and the CB1R tone is dysregulated in obesity. This study aimed to investigate CB1R availability in peripheral tissue and brain in young men with overweight versus lean men.

Methods: Healthy males with high (HR, $n = 16$) or low (LR, $n = 20$) obesity risk were studied with fluoride 18-labeled FMPEP- d_2 positron emission tomography to quantify CB1R availability in abdominal adipose tissue, brown adipose tissue, muscle, and brain. Obesity risk was assessed by BMI, physical exercise habits, and familial obesity risk, including parental overweight, obesity, and type 2 diabetes. To assess insulin sensitivity, fluoro-[^{18}F]-deoxy-2-D-glucose positron emission tomography during hyperinsulinemic-euglycemic clamp was performed. Serum endocannabinoids were analyzed.

Results: CB1R availability in abdominal adipose tissue was lower in the HR than in the LR group, whereas no difference was found in other tissues. CB1R availability of abdominal adipose tissue and brain correlated positively with insulin sensitivity and negatively with unfavorable lipid profile, BMI, body adiposity, and inflammatory markers. Serum arachidonoyl glycerol concentration was associated with lower CB1R availability of the whole brain, unfavorable lipid profile, and higher serum inflammatory markers.

Conclusions: The results suggest endocannabinoid dysregulation already in the pre-obesity state.

INTRODUCTION

The number of people with obesity is increasing worldwide [1]. Obesity is a complex disease characterized by excess adipose tissue accumulation increasing the risk for other diseases and metabolic abnormalities [2]. Because of the significant burden to individuals and community due to obesity, effective tools for preventing and treating obesity are needed.

The endocannabinoid system (ECS) plays a central role in regulating food intake, energy homeostasis, and lipid metabolism at both the central and peripheral level [3, 4]. ECS consists of two G protein-coupled receptors: cannabinoid type 1 and type 2 (CB1R and CB2R, respectively) receptors, their ligands endocannabinoids, and the ligand-metabolizing enzymes [4]. CB1Rs, which are essential in energy homeostasis, are widely expressed in the central nervous system, notably in brain regions controlling energy balance and feeding behavior such as the hypothalamus, corticolimbic circuits, ventral tegmental area, and brain stem [5, 6]. Peripherally, CB1Rs are expressed in tissues controlling energy homeostasis, including gastrointestinal tract, adipose tissue, liver, skeletal muscle, and endocrine pancreas.

Endocannabinoids, of which the most studied are anandamide (AEA) and 2-arachidonoylglycerol (2-AG), act as ligands to CB1Rs, which exert a cascade promoting energy preservation leading to increased food intake, adipose tissue accumulation, increased levels of proinflammatory markers, decreased energy expenditure and thermogenesis, insulin resistance, and weight gain [3–7]. Endocannabinoids are synthesized and released locally on demand under tight regulation by neurons [3, 4]. During a prolonged metabolic dysregulation, however, the ECS tone can become upregulated; CB1R upregulation and increased levels of endocannabinoids in brain, peripheral tissue, and circulation have been found in animals and humans with obesity [7, 8].

Antagonism of CB1Rs contributes to reductions of food intake, body weight, adiposity, insulin resistance, and plasma triglycerides and an increase in the high-density lipoprotein (HDL)/low-density lipoprotein (LDL) cholesterol ratio [4, 7, 8]. After withdrawal of the first CB1R inverse agonist rimonabant (SR141716) from clinical use because of its neuropsychiatric side effects, therapeutic strategies targeting the peripheral ECS have been investigated. In murine models, peripherally restricted CB1R antagonists or inverse agonists and allosteric inhibitors of CB1Rs, compounds decreasing endocannabinoid synthesis or increasing endocannabinoid degradation, have been shown to have beneficial effects by reducing food intake, weight, hyperleptinemia, insulin resistance, and dyslipidemia without central side effects [6, 9].

Recently, we found no significant difference in CB1R availability in brain of healthy lean males versus males with overweight studied using positron emission tomography (PET) imaging and CB1R inverse agonist radioligand fluoride 18-labeled FMPEP- d_2 ([3R,5R]-5-[3-methoxy-phenyl]-3-[[R]-1-phenyl-ethylamino]-1-[4-trifluoro-methyl-phenyl]-pyrrolidin-2-one). However, BMI and parental history of overweight, obesity, and type 2 diabetes (T2D) had a negative association with CB1R availability [10]. Here, we investigated CB1R availability in peripheral tissues and in the whole brain in the same sample with [18 F]FMPEP- d_2 PET imaging [11] and compared the tissue CB1R availability with insulin sensitivity, body adiposity, and related cardiometabolic risk factors and circulating endocannabinoid levels. We found

Study Importance

What is already known?

- Cannabinoid type 1 receptors (CB1Rs) participate in the control of energy balance and lipid and glucose metabolism at the central and peripheral level, and obesity is associated with dysregulation of the endocannabinoid system.
- CB1R availability can be studied *in vivo* using positron emission tomography (PET) imaging and CB1R inverse agonist radioligand [18 F]FMPEP- d_2 .

What does this study add?

- We found lower abdominal adipose tissue CB1R availability in young men with overweight, as compared with lean men, and an association between lower CB1R availability and decreased insulin sensitivity, unfavorable lipid profile, and higher body adiposity and inflammatory markers.
- Whole-brain CB1R availability did not differ between the groups, but lower cerebral CB1R availability was associated with decreased whole-body insulin sensitivity and higher body adiposity.

How might these results change the direction of research or the focus of clinical practice?

- The study findings provide further knowledge about the endocannabinoid system dysregulation that may take place already in the preobesity state and encourage further effort for investigating CB1Rs as a target to treat obesity and metabolic disorders.

that obesity risk was associated with lowered CB1R availability in abdominal adipose tissue, which, in turn, was associated with decreased insulin sensitivity, unfavorable lipid profile, and higher weight, BMI, body adiposity, and inflammatory markers.

METHODS

Study participants

We studied 21 healthy young male participants with low (LR) and 16 with high (HR) obesity risk. A detailed description of the recruitment, inclusion, and exclusion criteria and a screening visit has been previously published [10]. Briefly, inclusion criteria for the LR group were male sex, age 20 to 35 years, BMI of 18.5 to 24.9 kg/m², leisure time physical activity ≥ 4 hours per week, and no parental overweight, obesity, or T2D. Inclusion criteria for the HR group were male sex, age 20 to 35 years, BMI of 25 to 30, leisure time physical activity < 4 hours per week, and parental overweight, obesity, or T2D. Overweight,

physical inactivity, and parental obesity and T2D have been established as risk factors for future obesity [12–17]. One HR participant's [^{18}F]FMPEP- d_2 uptake in brown adipose tissue (BAT) was not possible to analyze reliably because of marked spillover from adjacent structures.

The sample size was determined by a priori power analysis based on earlier PET studies on obesity [18] suggesting that a sample size of 16 + 16 would be sufficient for power of 0.95 at $p < 0.05$, assuming effect size (r) = 0.5. Each participant provided written informed consent. The study protocol was approved by the Ethics Committee of the Hospital District of Southwest Finland and conducted in accordance with the principles of the Declaration of Helsinki. The study is a part of the PROSPECT project registered at ClinicalTrials.gov (Neuromolecular Risk Factors for Obesity, PROSPECT, NCT03106688).

Study design

CB1R availability was measured with dynamic PET/computed tomography (CT) using the CB1R inverse agonist radioligand [^{18}F]FMPEP- d_2 . Tissue glucose uptake (GU) rates were determined with fluoro-[^{18}F]-deoxy-2-D-glucose (FDG) PET/CT during a hyperinsulinemic-euglycemic clamp. Whole-body insulin sensitivity (M value) and endogenous glucose production (EGP) were calculated. Magnetic resonance imaging (MRI) was conducted to assess abdominal subcutaneous (SAT) and visceral (VAT) adipose tissue masses. PET/CT and MRI studies were performed at room temperature on separate days at the Turku PET Centre, Finland. Body fat mass percentage was measured with an air displacement plethysmograph (the Bod Pod system, software version 5.4.0, COSMED, Inc.) after at least 4 hours of fasting. Serum endocannabinoid levels and metabolic biomarkers were quantified.

Radiochemistry

The radioligand [^{18}F]FMPEP- d_2 was synthesized according to the standard operating procedure of the Turku PET Centre as previously described [10, 19]. FDG was produced using the FASTlab synthesis platform (GE Healthcare) according to the modified method of Hamacher et al. [20] and Lemaire et al. [21].

[^{18}F]FMPEP- d_2 PET/CT scanning protocol

[^{18}F]FMPEP- d_2 PET images were acquired with PET/CT (GE Discovery VCT PET/CT, GE Healthcare) after a 6- to 12-hour fast. The study protocol has been described in detail in our previous report [10]. In brief, two catheters were inserted in veins of opposite forearms, one for blood sampling and one for [^{18}F]FMPEP- d_2 injection. Blood samples were collected to measure hematocrit and serum endocannabinoid concentrations before the scan. A heating pillow was used on the arm to obtain arterialized blood samples. Then 147 to 215 MBq of [^{18}F]FMPEP- d_2 was injected intravenously, and dynamic scans of the brain (60 minutes), neck (12 minutes), and

abdomen (9 minutes) and a late scan of the brain were conducted. CT scans of each region were performed for photon attenuation and anatomical reference. Arterialized venous blood samples were drawn on the opposite arm from the injection site to measure plasma radioactivity and [^{18}F]FMPEP- d_2 radio-metabolites. Radioactivity was measured with an automatic gamma counter (Wizard 1480 3", Wallac).

[^{18}F]FMPEP- d_2 PET/CT image analysis

CB1R availability of tissues was quantified from [^{18}F]FMPEP- d_2 PET/CT images by determining fractional uptake rate (FUR) and volume distribution (V_T) of the radioligand as previously described [11]. Carimas Software (version 2.9, Turku PET Centre, <https://turkupetcentre.fi/software/>) was used for image analysis of SAT, intraperitoneal white adipose tissue (IWAT) and retroperitoneal white adipose tissue (RWAT), BAT, and muscle. Regions of interest (ROI) were manually drawn on the fused PET/CT images to several volumes of abdominal SAT, IWAT, and RWAT. BAT ROIs were drawn bilaterally in supraclavicular adipose tissue depots. For ROIs of adipose tissue, only voxels of Hounsfield units (HU) within the range of –50 to –250 HU were included [22]. Muscle ROIs were drawn bilaterally in the deltoid muscle. To limit the effect of spillover due to partial volume effect and motion, several ROIs in several slices of images for each tissue were drawn avoiding large vessels. Radio-metabolite corrected plasma input for image analysis was determined by correcting the acquired plasma time-activity curve (TAC) with the parent tracer fraction measured using thin layer chromatography and digital autoradiography as previously described [6].

FUR of the [^{18}F]FMPEP- d_2 in each peripheral tissue was calculated by dividing the tissue radioactivity concentration at time X by the Area Under the Curve_{0-X} of the radio-metabolite corrected plasma TAC. V_T of each peripheral tissue was calculated by dividing the radioactivity concentration in tissue by radio-metabolite corrected plasma TAC, whereas the tissue scans were performed as late scans. V_T of the [^{18}F]FMPEP- d_2 in the whole brain was determined by applying the reversible one-tissue compartmental model using the radio-metabolite corrected plasma TAC as model input as presented earlier [10, 11, 23]. Mean V_T of brain was computed as the average of all white and gray matter voxels within the Montreal Neurological Institute (MNI) space template.

FDG PET/CT scanning protocol and image analysis

The FDG PET/CT scanning protocol has been detailed in our previous report [10]. Studies were done after a 12-hour overnight fast with the GE Discovery (Discovery 690 PET/CT, GE Healthcare) PET camera. Hyperinsulinemic-euglycemic clamp was applied as previously described [24] in order to measure whole-body insulin sensitivity. A detailed description of the FDG PET/CT scanning protocol, hyperinsulinemic-euglycemic clamp execution, PET/CT image analysis, determination of plasma input, quantification of tissue-specific GU rates, and measurement of EGP is available in the online Supporting Information.

TABLE 1 Characteristics of the study participants in the LR and HR groups

	LR (n = 21)	HR (n = 16)	p value
Age (y)	23 ± 3	28 ± 4	0.0008
Weight (kg)	70.6 ± 7.6	92.1 ± 7.9	<0.0001
BMI (kg/m ²)	22.1 ± 2.0	27.3 ± 1.9	<0.0001
Body fat mass (kg)	11.9 ± 4.3	28.4 ± 8.9	<0.0001
Body fat mass (%)	16.7 ± 5.4	30.0 ± 7.9	<0.0001
Fat-free mass (kg)	59.2 ± 6.8	63.8 ± 5.3	0.03
Abdominal SAT mass (kg)	2.8 ± 1.0	7.2 ± 2.4	<0.0001
VAT mass (kg)	1.4 ± 0.8	3.8 ± 1.2	<0.0001
Systolic blood pressure (mm Hg)	124 ± 12	135 ± 12	0.008
Diastolic blood pressure (mm Hg)	76 ± 10	82 ± 9	0.08
<i>Fasting</i>			
Plasma glucose (mmol/L)	4.9 ± 0.5	5.5 ± 0.4	0.0004
Plasma insulin (pmol/L)	38.7 ± 21.2	63.9 ± 22.3	0.001
Serum FFA (mmol/L)	0.30 ± 0.11	0.32 ± 0.14	0.8
<i>2-Hour OGTT</i>			
Plasma glucose (mmol/L)	4.7 ± 1.0	6.0 ± 1.4	0.002
Plasma insulin (pmol/L)	163.7 ± 144.5	360.9 ± 244.3	0.004
HbA _{1c} (mmol/mol)	29 ± 2	32 ± 3	0.0008
HbA _{1c} (%)	4.8 ± 0.2	5.1 ± 0.3	0.001
hs-CRP (mg/L)	0.4 ± 0.3	1.2 ± 1.1	0.001
M value (μmol/kg/min)	57.0 ± 14.2	36.5 ± 12.0	<0.0001
M value (μmol/kg _{FFM} /min)	68.8 ± 17.3	50.4 ± 13.7	0.001
Rd (μmol/kg/min)	50.7 ± 10.6	35.7 ± 10.0	0.0001
Rd (μmol/kg _{FFM} /min)	61.1 ± 11.6	50.8 ± 11.0	0.01
EGP (μmol/kg/min) ^a	−3.3 ± 6.8	0.6 ± 4.7	0.06
EGP (μmol/kg _{FFM} /min) ^a	−2.0 ± 9.1	1.4 ± 7.2	0.2
Clamp serum FFA (mmol/L)	0.03 ± 0.01	0.05 ± 0.03	0.6
<i>Glucose uptake (μmol/100 g/min)</i>			
Abdominal SAT	2.2 ± 0.8	1.2 ± 0.6	0.0001
VAT	3.2 ± 0.7	1.9 ± 0.6	<0.0001
BAT ^b	3.1 ± 0.8	2.3 ± 0.9	0.005
Muscle ^c	5.1 ± 1.3	3.3 ± 0.9	<0.0001
Femoral SAT ^c	1.9 ± 0.7	1.2 ± 0.6	0.001
Liver	2.5 ± 0.6	2.1 ± 0.7	0.09

Note: Data presented as mean ± SD.

Abbreviations: BAT, brown adipose tissue; EGP, endogenous glucose production; FFA, free fatty acids; FFM, fat-free mass; HbA_{1c}, glycated hemoglobin; HR, high risk; hs-CRP, high-sensitivity C-reactive protein; LR, low risk; M value, whole-body insulin sensitivity; OGTT, oral glucose tolerance test; Rd, rate of disappearance of glucose; SAT, subcutaneous adipose tissue; VAT, visceral adipose tissue.

^aMean and SD for the LR (n = 20) and HR (n = 16) participants who gave a urine sample.

^bMean and SD for the LR (n = 20) and HR (n = 16) participants who completed the FDG scan successfully.

^cMean and SD for the LR (n = 19) and HR (n = 16) participants who completed the FDG scan successfully.

Biochemical analysis

A detailed description of the methods of the biochemical analysis of plasma glucose and insulin and serum free fatty acids (FFA) and high-sensitivity C-reactive protein is provided in the online Supporting Information. Metabolic biomarkers were quantified from serum

from 19 LR and 16 HR subjects at fasting using high-throughput proton nuclear magnetic resonance (NMR) [25] metabolomics (Nightingale Health Oyj, Helsinki, Finland). Eight different serum endocannabinoids and related structures were measured: arachidonic acid, AEA, 1- and 2-arachidonoyl glycerol (AG 1 + 2), α-linolenic acid (α-LEA), γ-linolenic acid (γ-LEA), docosatetraenoyl ethanolamide

TABLE 2 Serum metabolic biomarkers in the LR and HR groups

	LR (n = 19)	HR (n = 16)	p value
<i>Cholesterol (mmol/L)</i>			
Total cholesterol	3.6 ± 0.4	4.5 ± 0.9	0.0008
Remnant cholesterol	1.0 ± 0.2	1.4 ± 0.4	0.001
VLDL cholesterol	0.4 ± 0.1	0.6 ± 0.2	0.0009
LDL cholesterol	1.3 ± 0.2	1.9 ± 0.5	<0.0001
HDL cholesterol	1.3 ± 0.2	1.2 ± 0.2	0.1
Total esterified cholesterol	2.6 ± 0.3	3.3 ± 0.6	0.0002
<i>Glycerides and phospholipids (mmol/L)</i>			
Total triglycerides	0.8 ± 0.2	1.3 ± 0.7	0.005
VLDL triglycerides	0.5 ± 0.2	1.0 ± 0.6	0.005
LDL triglycerides	0.09 ± 0.01	0.1 ± 0.03	0.001
HDL triglycerides	0.07 ± 0.02	0.09 ± 0.03	0.06
Phosphoglycerides	2.0 ± 0.2	2.2 ± 0.4	0.03
Ratio of triglycerides to phosphoglycerides	0.4 ± 0.1	0.6 ± 0.2	0.005
Total cholines	2.3 ± 0.2	2.5 ± 0.4	0.03
Phosphatidylcholines	1.9 ± 0.2	2.1 ± 0.4	0.03
Sphingomyelins	0.4 ± 0.04	0.4 ± 0.05	0.002
<i>Apolipoproteins (g/L)</i>			
ApoB	0.6 ± 0.1	0.8 ± 0.2	0.0002
ApoA1	1.3 ± 0.2	1.3 ± 0.1	0.7
ApoB/ApoA1	0.5 ± 0.1	0.6 ± 0.2	0.0003
<i>Fatty acids (mmol/L)</i>			
Total fatty acids	9.4 ± 1.0	11.6 ± 2.7	0.003
Omega-3 fatty acids	0.4 ± 0.1	0.5 ± 0.2	0.1
Omega-6 fatty acids	4.0 ± 0.3	4.5 ± 0.6	0.004
PUFA	4.4 ± 0.4	5.0 ± 0.8	0.006
MUFA	2.2 ± 0.3	3.0 ± 0.9	0.002
Saturated fatty acids	2.8 ± 0.4	3.7 ± 1.1	0.004
Linoleic acid	3.5 ± 0.3	4.0 ± 0.6	0.003
Docosahexaenoic acid	0.2 ± 0.1	0.3 ± 0.05	0.3
<i>Fatty acids (% of total fatty acids)</i>			
Omega-3 fatty acids	4.4 ± 1.4	4.2 ± 0.8	0.7
Omega-6 fatty acids	42.3 ± 1.7	39.3 ± 3.7	0.004
PUFA	46.7 ± 2.2	43.6 ± 3.4	0.003
MUFA	23.4 ± 2.0	25.2 ± 1.8	0.01
Saturated fatty acids	29.9 ± 1.5	31.3 ± 2.3	0.04
Linoleic acid	37.5 ± 1.8	35.3 ± 3.5	0.03
Docosahexaenoic acid	2.5 ± 0.6	2.2 ± 0.3	0.1
<i>Ketone bodies (mmol/L)</i>			
3-Hydroxybutyrate	0.05 ± 0.05	0.04 ± 0.03	0.2
Acetate	0.07 ± 0.03	0.05 ± 0.02	0.02
Acetoacetate	0.05 ± 0.03	0.04 ± 0.02	0.2
Acetone	0.02 ± 0.01	0.02 ± 0.01	0.1
<i>Glycolysis related metabolites (mmol/L)</i>			
Glucose	4.9 ± 0.1	5.4 ± 0.4	<0.0001
Lactate	1.8 ± 0.3	2.1 ± 0.4	0.02

(Continues)

TABLE 2 (Continued)

	LR (n = 19)	HR (n = 16)	p value
Pyruvate	0.1 ± 0.02	0.08 ± 0.03	0.05
Citrate	0.1 ± 0.01	0.06 ± 0.01	0.5
<i>Amino acids (mmol/L)</i>			
Alanine	0.3 ± 0.1	0.3 ± 0.1	0.1
Glutamine	0.8 ± 0.1	0.8 ± 0.1	0.5
Glycine	0.3 ± 0.1	0.2 ± 0.03	0.2
Histidine	0.1 ± 0.01	0.08 ± 0.01	0.5
<i>Branched-chain amino acids</i>			
Isoleucine	0.1 ± 0.02	0.1 ± 0.01	0.5
Leucine	0.1 ± 0.02	0.1 ± 0.01	0.07
Valine	0.2 ± 0.04	0.3 ± 0.03	0.4
<i>Aromatic amino acids</i>			
Phenylalanine	0.06 ± 0.01	0.06 ± 0.01	0.2
Tyrosine	0.06 ± 0.01	0.07 ± 0.01	0.4
<i>Fluid balance</i>			
Creatinine (μmol/L)	76.8 ± 10.1	82.9 ± 10.5	0.09
Albumin (g/L)	41.5 ± 2.4	41.9 ± 2.3	0.7
<i>Inflammation (mmol/L)</i>			
GlycA	0.7 ± 0.1	0.8 ± 0.1	<0.0001

Note: Data presented as mean ± SD. Serum samples of 35 participants (19 LR and 16 HR participants) were analyzed.

Abbreviations: ApoA1, apolipoprotein A1; ApoB, apolipoprotein B; GlycA, glycoprotein acetyls; HDL, high-density lipoprotein; HR, high risk; LDL, low-density lipoprotein; LR, low risk; MUFA, monounsaturated fatty acids; PUFA, polyunsaturated fatty acids; VLDL, very low-density lipoprotein.

(DEA), *N*-arachidonoyl-L-serine, and oleyl ethanolamide. Because of rapid isomerization of 1-AG and 2-AG at room temperature, a total concentration of AG (1 + 2) was reported. Fasting-state blood samples collected during the [¹⁸F]FMPEP-*d*₂ study day were used and analyzed as previously described [10, 26].

Measurement of tissue masses

The abdominal SAT and VAT masses were analyzed from MRI images using sliceOmatic (Tomovision). A detailed description of the tissue mass analyses is provided in the online Supporting Information.

Statistical methods

Data are presented as mean ± SD. Between-group comparisons were performed with independent samples *t* test or Wilcoxon rank sum test as appropriate. Categorical variables were compared with χ^2 test. Statistical analyses were performed with SPSS Statistics software, version 28.0 (IBM Corp.). Associations between study variables were tested using Pearson or Spearman correlation tests. *P* values < 0.05 were considered statistically significant.

RESULTS

Participant characteristics

The HR participants had higher weight, BMI, total body fat mass, and abdominal SAT and VAT masses than the LR participants. The HR group also had worse glycemic profiles and lower insulin-stimulated tissue-specific GU rates and *M* values compared with the LR group, indicating lower insulin sensitivity; however, insulin-suppressed EGP did not differ between the groups. High-sensitivity C-reactive protein level was higher in the HR than in the LR group. The HR participants were older than the LR group (Table 1). Serum metabolite levels were higher in the HR group for total, remnant, very low-density lipoprotein (VLDL), and LDL cholesterol, triglycerides, apolipoprotein B (ApoB), ApoB/ApoA1 ratio, and fatty acids than in the LR group. Also, glycoprotein acetyls (GlycA), a biomarker of systemic inflammation, was higher in the HR than in the LR group (Table 2).

Lower CB1R availability in abdominal adipose tissue in the HR than in the LR group

The HR group exhibited lower FUR and *V_T* of the [¹⁸F]FMPEP-*d*₂ in abdominal SAT, IWAT, and RWAT, indicating lower CB1R availability as compared with the LR group. The muscle FUR and *V_T* were numerically

lower in the HR than in the LR group but this did not reach statistical significance. No difference was found in CB1R availability of BAT and the whole brain between the groups (Figure 1). As the V_T and FUR of $[^{18}\text{F}]\text{FMPEP-d}_2$ are both assumed to represent CB1R availability in tissue, the V_T and FUR values in each tissue correlated positively with each other ($r = 0.80$, $p < 0.0001$ for abdominal SAT; $r = 0.72$, $p < 0.0001$ for IWAT; $r = 0.78$, $p < 0.0001$ for RWAT; $r = 0.87$, $p < 0.0001$ for BAT; $r = 0.58$, $p = 0.0002$ for muscle). Intertissue associations of CB1R availability are presented in Supporting Information Table S1.

Association between CB1R availability and insulin sensitivity

When comparing the tissue CB1R availability with tissue-specific GU rates, we found a positive association between the two in abdominal adipose tissue (Table 3 and Figure 2A–C). CB1R availability of IWAT and RWAT correlated positively also with BAT, skeletal muscle, and femoral SAT GU, and CB1R availability of SAT with femoral SAT GU. CB1R availability of BAT correlated positively only with VAT GU.

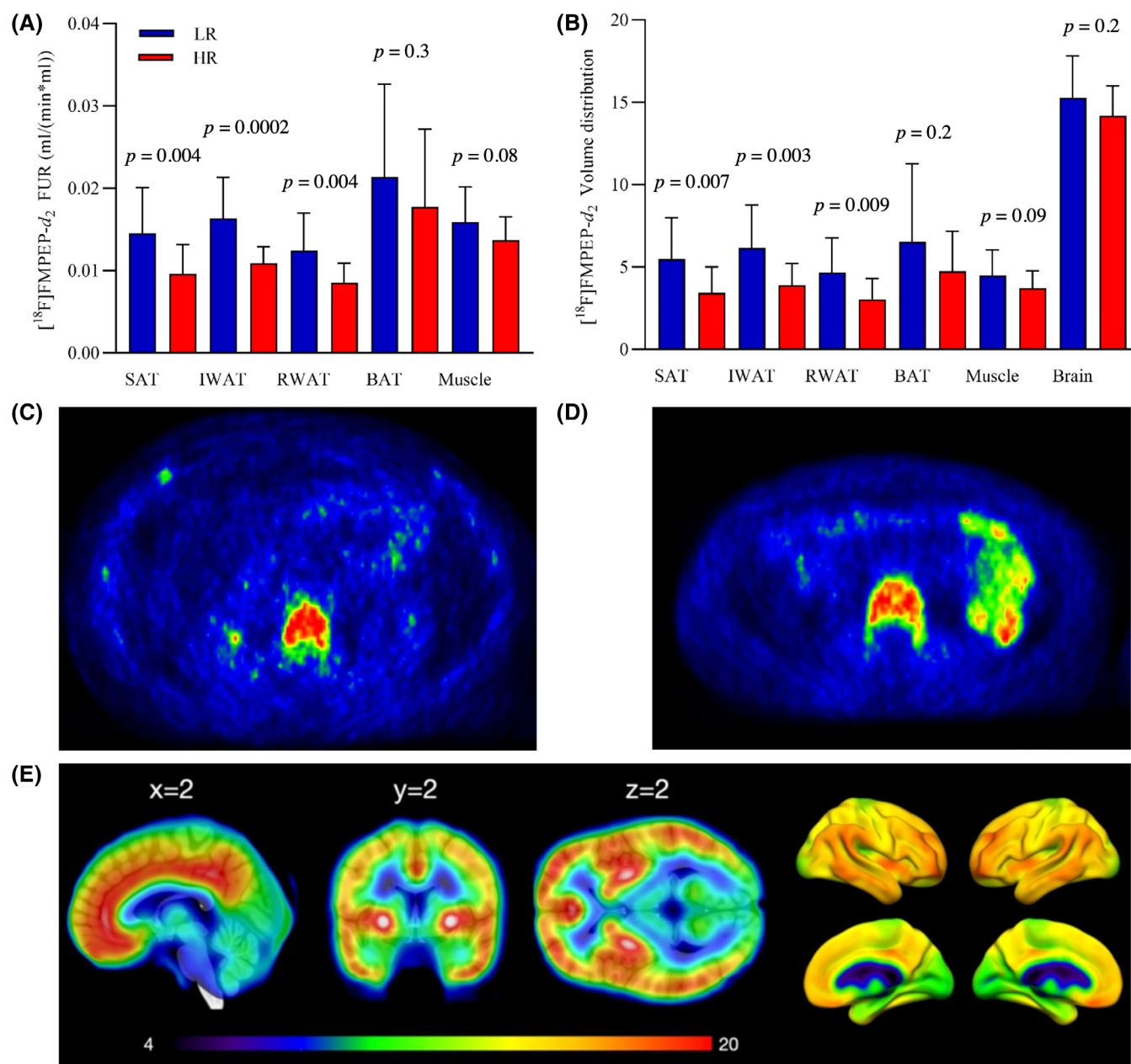


FIGURE 1 Lower CB1R availability in abdominal SAT, IWAT, and RWAT in the HR as compared with the LR group. (A) FUR of $[^{18}\text{F}]\text{FMPEP-d}_2$ in abdominal SAT, IWAT, RWAT, BAT, and muscle in the LR and HR groups. (B) $[^{18}\text{F}]\text{FMPEP-d}_2$ volume distribution (V_T) of SAT, IWAT, RWAT, BAT, muscle, and the whole brain in the LR and HR groups. PET abdomen images depicting FUR of $[^{18}\text{F}]\text{FMPEP-d}_2$ of (C) one HR and (D) one LR participant. (E) Mean V_T for the $[^{18}\text{F}]\text{FMPEP-d}_2$ scans. BAT, brown adipose tissue; FUR, fractional uptake rate; HR, high risk; IWAT, intraperitoneal white adipose tissue; LR, low risk; RWAT, retroperitoneal white adipose tissue; SAT, subcutaneous adipose tissue

CB1R availability of muscle and the whole brain correlated positively only with BAT GU (Table 3).

Considering whole-body insulin sensitivity, we found a positive correlation between CB1R availability of RWAT and M value and the rate of disappearance of glucose (Rd), and CB1R availability of IWAT and Rd. CB1R availability of the whole brain correlated positively with M value and negatively with insulin-suppressed EGP adjusted with fat-free mass (EGP_{FFM}; Table 3 and Supporting Information Figure S1). CB1R availability of abdominal adipose tissue depots correlated negatively with serum insulin-suppressed FFA level (Table 3).

Association between CB1R availability and body composition

CB1R availability of abdominal adipose tissue depots correlated negatively with weight, BMI, total body fat, and abdominal SAT and VAT masses. CB1R availability of muscle correlated negatively with weight, BMI, VAT mass, and FFM. CB1R availability of the whole brain correlated negatively with weight, BMI, total body fat mass, and VAT mass. CB1R availability of BAT did not correlate with any of these measures (Table 3).

TABLE 3 Associations between [¹⁸F]FMPEP-d₂ FUR values of abdominal SAT, IWAT, RWAT, BAT, and muscle and V_T of the whole brain and anthropometric and metabolic characteristics and insulin-stimulated tissue-specific glucose uptake rates

	[¹⁸ F]FMPEP-d ₂ FUR (mL/[min × mL])					
	SAT	IWAT	RWAT	BAT	Muscle	V _T Brain
Age (y)	−0.31	−0.42**	−0.42**	−0.16	−0.33*	−0.24
Weight (kg)	−0.49**	−0.59***	0.57***	−0.25	−0.40*	−0.39*
BMI (kg/m ²)	−0.49**	−0.57***	−0.59***	−0.29	−0.40*	−0.44**
Body fat mass (kg)	−0.56***	−0.63***	−0.65***	−0.13	−0.31	−0.36*
Body fat mass (%)	−0.53***	−0.63***	−0.68***	−0.07	−0.25	−0.36*
Fat-free mass (kg)	−0.15	−0.16	−0.09	−0.32	−0.35*	−0.08
Abdominal SAT mass (kg)	−0.55***	−0.60**	−0.59***	−0.09	−0.29	−0.28
VAT mass (kg)	−0.50**	−0.66***	−0.60***	−0.10	−0.33*	−0.37*
Systolic blood pressure (mm Hg)	−0.19	−0.34*	−0.35*	0.11	−0.10	−0.50**
Diastolic blood pressure (mm Hg)	−0.07	−0.23	−0.22	0.15	−0.17	−0.42**
HbA _{1c} (mmol/mol)	−0.23	−0.37*	−0.20	−0.004	0.09	−0.10
hs-CRP (mg/L)	−0.32	−0.31	−0.26	−0.07	−0.17	−0.28
Fasting serum FFA (mmol/L)	0.078	−0.04	−0.10	0.14	−0.02	−0.25
Clamp serum FFA (mmol/L)	−0.39*	−0.39*	−0.38*	−0.007	−0.13	−0.31
M value (μmol/kg/min)	0.28	−0.27	0.39*	0.17	0.19	0.38*
M value (μmol/kg _{FFM} /min)	0.16	0.14	0.24	0.17	0.16	0.35*
Rd (μmol/kg/min)	0.26	0.36*	0.42*	0.14	0.20	0.23
Rd (μmol/kg _{FFM} /min)	0.15	0.20	0.28	0.14	0.18	0.24
EGP (μmol/kg/min) ^a	−0.05	0.08	0.02	0.10	0.06	−0.33
EGP (μmol/kg _{FFM} /min) ^a	−0.12	−0.01	−0.08	0.08	0.05	−0.43*
Glucose uptake (μmol/100 g/min)						
Abdominal SAT	0.56***	0.64***	0.60***	0.31	0.24	0.30
VAT	0.57***	0.67***	0.62***	0.37*	0.32	0.32
BAT ^b	0.33	0.43*	0.50**	0.03	0.34*	0.34*
Muscle ^c	0.25	0.34*	0.41*	0.18	0.21	0.20
Femoral SAT ^c	0.41*	0.45**	0.51**	0.03	0.11	0.34
Liver	0.15	−0.002	0.02	0.09	−0.02	−0.23

Note: Data are Pearson *r* values. Significant associations are indicated by bold font.

Abbreviations: BAT, brown adipose tissue; EGP, endogenous glucose production; FFA, free fatty acids; FFM, fat-free mass; FUR, fractional uptake rate; HbA_{1c}, glycated hemoglobin; HR, high risk; hs-CRP, high-sensitivity C-reactive protein; IWAT, intraperitoneal white adipose tissue; LR, low risk; M value, whole-body insulin sensitivity; Rd, rate of disappearance of glucose; RWAT, retroperitoneal white adipose tissue; SAT, subcutaneous adipose tissue; VAT, visceral adipose tissue; V_T, volume distribution.

^aAssociations with the LR (*n* = 20) and HR (*n* = 16) participants who gave a urine sample.

^bAssociations with the LR (*n* = 20) and HR (*n* = 16) participants who completed the FDG scan successfully.

^cAssociations with the LR (*n* = 19) and HR (*n* = 16) participants who completed the FDG scan successfully.

**p* < 0.05.

***p* < 0.01.

****p* < 0.001.

*****p* < 0.0001.

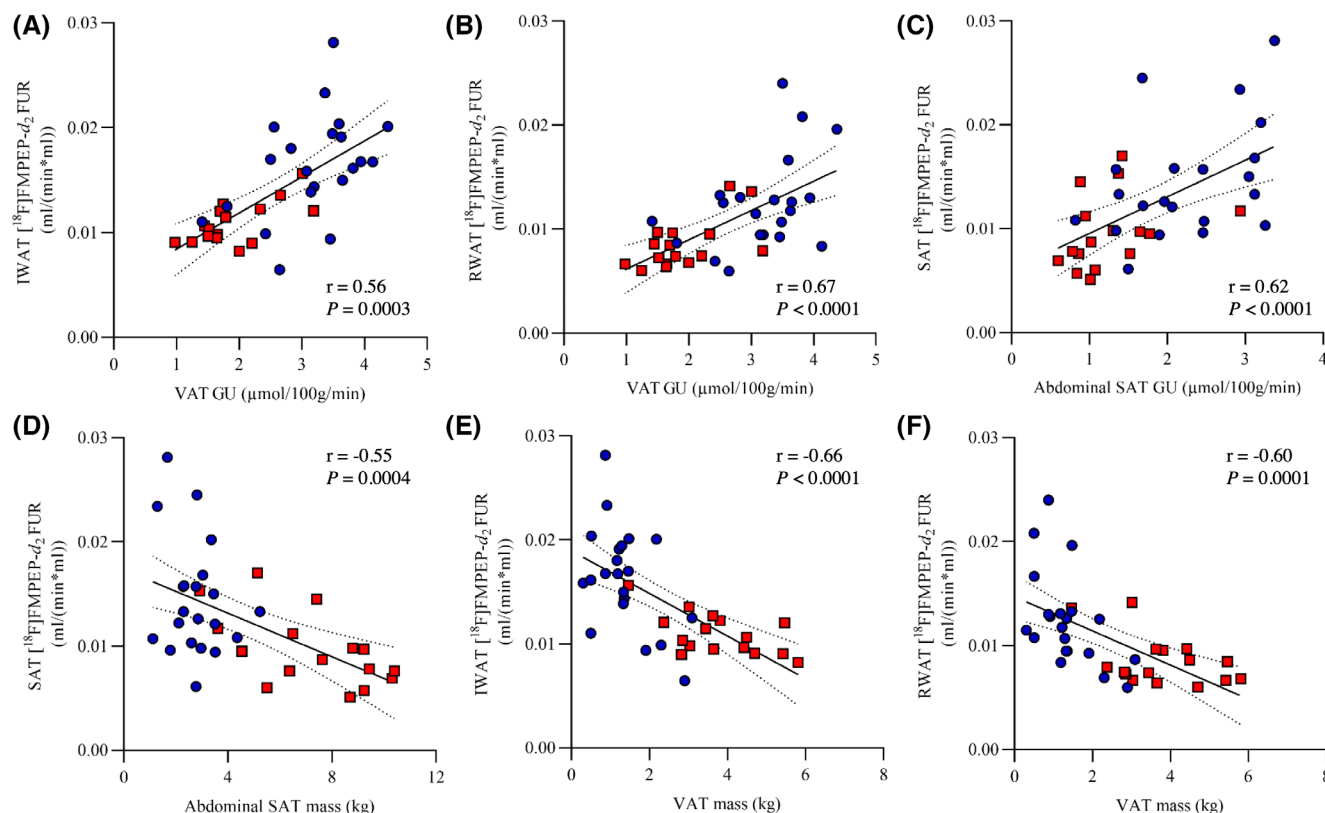


FIGURE 2 Associations between abdominal adipose tissue CB1R availability and tissue GU rates and tissue masses. Pearson correlation between $[^{18}\text{F}]\text{FMPEP-d}_2\text{ FUR}$ values of (A) abdominal SAT and SAT GU, (B) intraperitoneal WAT and VAT GU, (C) retroperitoneal WAT and VAT GU, (D) abdominal SAT and abdominal SAT mass, (E) intraperitoneal WAT and VAT mass, and (F) retroperitoneal WAT and VAT mass in the LR (blue circle) and HR (red square) groups. FUR, fractional uptake rate; GU, glucose uptake; HR, high risk; IWAT, intraperitoneal white adipose tissue; LR, low risk; RWAT, retroperitoneal white adipose tissue; SAT, subcutaneous adipose tissue; VAT, visceral adipose tissue

Association between CB1R availability and serum metabolomics

Lower CB1R availability in abdominal adipose tissue, muscle, and the whole brain was associated with unfavorable lipid profile (Figure 3). CB1R availability of abdominal adipose tissue depots and the whole brain correlated negatively with total, non-HDL, remnant, VLDL, and LDL cholesterol, triglycerides, free cholesterol, ratio of triglycerides to phosphoglycerides, ApoB, and ApoB/ApoA1 ratio. CB1R availability of IWAT, RWAT, and brain also correlated negatively with fatty acids, including omega-6 fatty acids and linoleic acid. CB1R availability of abdominal SAT correlated positively with HDL cholesterol. CB1R availability of muscle correlated negatively with total, non-HDL, remnant, VLDL, and LDL cholesterol, ApoB, ApoB/ApoA1 ratio, and fatty acids. CB1R availability of abdominal adipose tissue depots and brain correlated negatively with GlycA. CB1R availability of BAT did not correlate with serum metabolomics.

Association between CB1R availability and serum endocannabinoid levels

Serum endocannabinoid levels did not differ between the groups as reported previously [10] (Supporting Information Table S3). CB1R availability in the whole brain correlated negatively with AG (1 + 2), whereas no significant association was found between the peripheral tissue CB1R availability and serum endocannabinoid levels (Table 4).

Associations between serum endocannabinoid levels and insulin sensitivity, body composition, and serum metabolomics

Serum arachidonic acid and AEA levels correlated negatively with M value_{FFM}, and AEA level also correlated negatively with M value, Rd, and Rd_{FFM}. Serum AG (1 + 2) and docosatetraenoyl ethanolamide

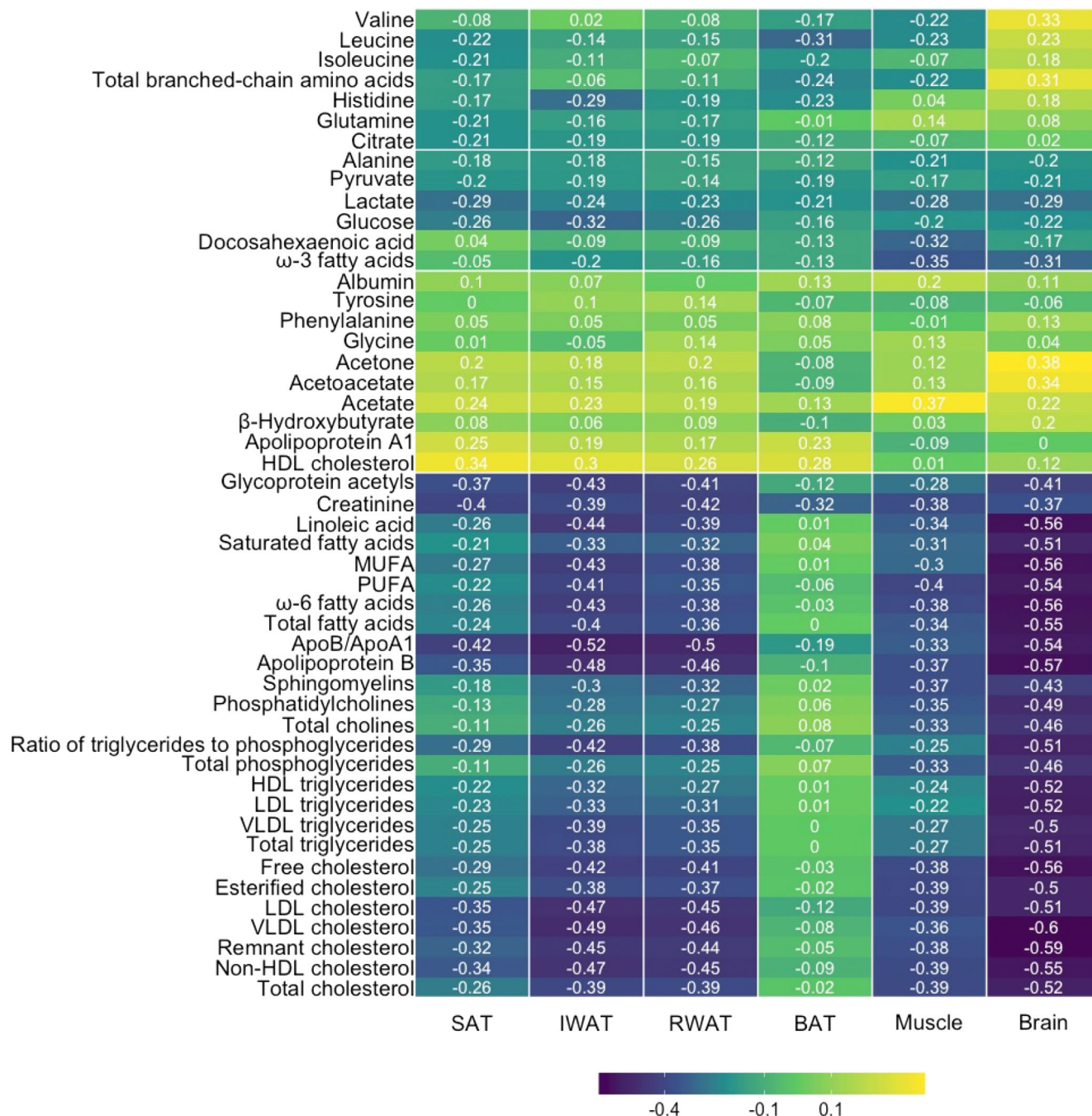


FIGURE 3 Correlation heat map between CB1R availability of abdominal SAT, IWAT, RWAT, BAT, muscle, and the whole brain with serum metabolomics across the whole study sample size. BAT, brown adipose tissue; IWAT, interperitoneal white adipose tissue; RWAT, retroperitoneal white adipose tissue; SAT, subcutaneous adipose tissue

levels correlated positively with EGP and EGP_{FFM}. No significant association was found between serum endocannabinoids and insulin-suppressed FFA levels. Regarding serum endocannabinoid levels and tissue-specific GU rates, γ-LEA was the only endocannabinoid to exhibit a significant correlation; serum γ-LEA correlated positively with abdominal SAT GU (Table 4).

Serum AG (1 + 2) level correlated positively with BMI. No association was found between serum endocannabinoid levels and weight or fat masses (Table 4).

Serum AG (1 + 2) level was associated with higher lipid levels including total, non-HDL, remnant, VLDL, and LDL cholesterol, as well as triglycerides, ApoB, ApoB/ApoA1 ratio, and fatty acids. AG (1 + 2) correlated positively also with Glyca. γ-LEA had a positive association with HDL cholesterol and ApoA1 (Figure 4).

Omega-6 polyunsaturated fatty acid linoleic acid correlated positively with abdominal SAT ($r = 0.40$, $p = 0.004$), VAT ($r = 0.60$, $p = 0.0001$), and total body fat ($r = 0.53$, $p = 0.001$) masses, weight ($r = 0.57$, $p = 0.0003$), and BMI ($r = 0.53$, $p = 0.001$). Omega-3 fatty

TABLE 4 Associations between circulating endocannabinoid concentrations and selected variables of body composition, insulin sensitivity, [^{18}F]FMPEP- d_2 FUR values of abdominal SAT, IWAT, and RWAT, BAT, and muscle, and [^{18}F]FMPEP- d_2 V_T of the whole brain

	AA	AEA	AG (1 + 2)	α -LEA	γ -LEA	DEA	NALS	OEA
Weight (kg)	0.04	0.23	0.26	0.16	0.14	0.09	-0.09	-0.06
BMI (kg/m ²)	0.16	0.22	0.36*	0.07	0.03	0.10	-0.08	-0.09
Body fat mass (kg)	0.06	0.24	0.23	0.02	-0.01	0.23	-0.08	0.02
Abdominal SAT mass (kg)	0.05	0.21	0.16	0.02	-0.04	0.24	-0.14	0.04
VAT mass (kg)	0.13	0.26	0.26	-0.02	-0.05	0.24	-0.06	0.09
M value ($\mu\text{mol/kg/min}$)	-0.31	-0.43**	-0.24	-0.16	-0.13	-0.33	-0.14	-0.26
M value ($\mu\text{mol/kg}_{\text{FFM}}/\text{min}$)	-0.34*	-0.44**	-0.23	-0.22	-0.20	-0.29	-0.18	-0.29
Rd ($\mu\text{mol/kg/min}$)	-0.25	-0.37*	-0.12	-0.02	-0.03	-0.22	-0.10	-0.19
Rd ($\mu\text{mol/kg}_{\text{FFM}}/\text{min}$)	-0.24	-0.43**	-0.03	-0.11	-0.12	-0.19	-0.06	-0.19
EGP ($\mu\text{mol/kg/min}$) ^a	0.28	0.24	0.40*	0.29	0.25	0.35*	0.29	0.26
EGP ($\mu\text{mol/kg}_{\text{FFM}}/\text{min}$) ^a	0.33	0.28	0.39*	0.22	0.22	0.41*	0.30	0.30
Clamp serum FFA (mmol/L)	0.03	0.02	0.02	-0.20	-0.15	0.04	-0.18	-0.10
Glucose uptake ($\mu\text{mol}/100\text{ g/min}$)								
Abdominal SAT	0.04	-0.10	-0.01	0.29	0.37*	-0.17	0.28	0.10
VAT	0.02	-0.12	-0.08	0.23	0.28	-0.26	0.14	-0.04
BAT ^b	-0.14	-0.33	0.10	0.08	0.08	-0.31	-0.03	-0.10
Muscle ^c	-0.19	-0.24	-0.06	-0.03	-0.01	-0.17	0.07	0.03
Femoral SAT ^c	0.00	0.01	-0.05	0.26	0.30	-0.05	0.22	0.22
Liver	0.23	0.01	0.23	-0.25	-0.13	-0.05	0.11	0.03
[^{18}F]FMPEP- d_2 FUR (mL/[min \times mL])								
SAT	0.24	-0.11	-0.15	0.25	0.32	-0.19	0.23	0.16
IWAT	0.19	-0.12	-0.22	0.26	0.22	-0.21	0.18	0.12
RWAT	0.19	-0.19	-0.20	0.25	0.25	-0.20	0.22	0.14
BAT ^d	-0.004	-0.07	-0.02	0.08	0.15	-0.06	-0.10	0.07
Muscle	-0.01	-0.26	-0.29	0.03	0.03	-0.11	0.09	-0.05
[^{18}F]FMPEP- d_2 V_T of the whole brain	-0.28	-0.20	-0.34*	0.03	-0.05	-0.03	-0.11	-0.03

Note: Data are Pearson r values. Significant associations are indicated by bold font.

Abbreviations: AA, arachidonic acid; AEA, anandamide; AG (1 + 2), arachidonoyl glycerol (1 + 2); α -LEA, α -linolenic acid; BAT, brown adipose tissue; DEA, docosatetraenoyl ethanolamide; EGP, endogenous glucose production; FFA, free fatty acids; FFM, fat-free mass; FUR, fractional uptake rate; IWAT, intraperitoneal white adipose tissue; γ -LEA, γ -linolenic acid; M value, whole-body insulin sensitivity; NALS, N-arachidonoyl-L-serine; OEA, oleyl ethanolamide; Rd, rate of disappearance of glucose; RWAT, retroperitoneal white adipose tissue; SAT, subcutaneous adipose tissue; VAT, visceral adipose tissue; V_T , volume distribution.

^aAssociations with the LR ($n = 20$) and HR ($n = 16$) participants who gave a urine sample.

^bAssociations with the LR ($n = 20$) and HR ($n = 16$) participants who completed the FDG scan successfully.

^cAssociations with the LR ($n = 19$) and HR ($n = 16$) participants who completed the FDG scan successfully.

^dAssociations with the LR ($n = 20$) and HR ($n = 16$) participants whose [^{18}F]FMPEP- d_2 image analysis was able to be conducted.

* $p < 0.05$.

** $p < 0.01$.

acids in turn correlated positively with AG (1 + 2; Figure 4) and negatively with CB1R availability of muscle (Figure 3).

DISCUSSION

Our main finding was that CB1R availability of abdominal adipose tissue was lower in young healthy patients with overweight and risk for obesity in comparison with lean patients. This suggests an impairment of peripheral ECS related to increased risk for developing obesity. Lower CB1R availability in abdominal adipose tissue was associated with

decreased adipose tissue and whole-body insulin sensitivity, unfavorable lipid profile, and higher body adiposity and inflammatory markers. Whole-brain CB1R availability did not differ between the groups, but lower cerebral CB1R availability was associated with decreased whole-body insulin sensitivity and higher body adiposity. Higher serum endocannabinoid levels were associated with decreased whole-body insulin sensitivity, unfavorable lipid profile, and higher serum inflammatory markers.

Only a few studies have quantified peripheral tissue CB1R availability in humans using [^{18}F]FMPEP- d_2 PET. A 2018 study [11] showed lower [^{18}F]FMPEP- d_2 binding in abdominal SAT, WAT, and brain in

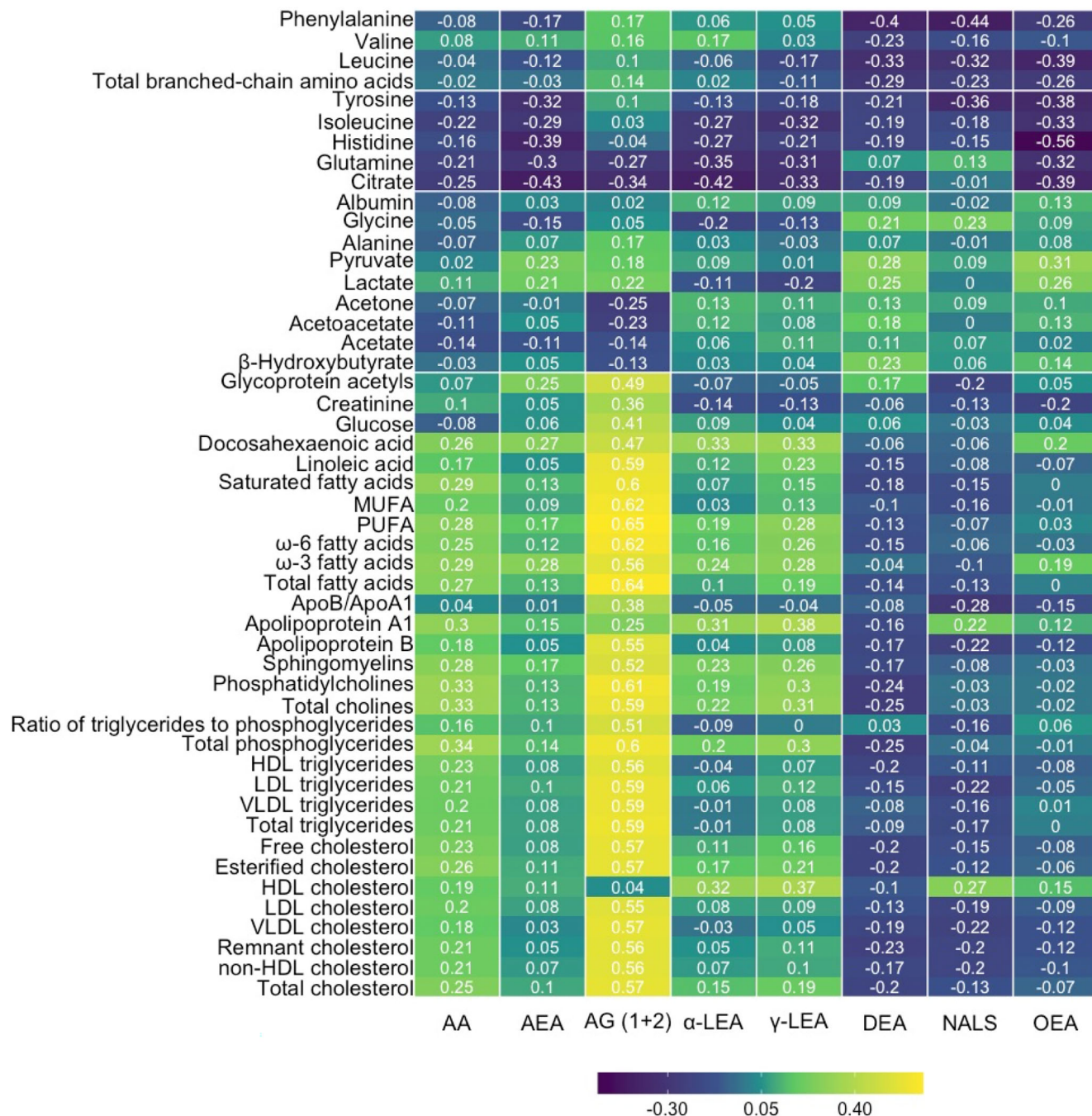


FIGURE 4 Correlation heat map between serum endocannabinoid levels and serum metabolomics across the whole study sample size. AA, arachidonic acid; AEA, anandamide; AG (1 + 2), arachidonoyl glycerol (1 + 2); α-LEA, α-linolenic acid; γ-LEA, γ-linolenic acid; DEA, docosatetraenoyl ethanolamide; NALS, N-arachidonoyl-L-serine; OEA, oleyl ethanolamide

healthy males with obesity (BMI: 32.9 ± 4.6) as compared with lean (BMI: 24.9 ± 1.7) males. Our study yielded converging results: lower CB1R availability in abdominal adipose tissue depots in the HR group than in the LR group. Compared with the previous report [11], the participants in the current study had overweight not obesity. This could contribute to the finding that CB1R availability of the whole brain did not differ between the groups, although lower CB1R availability was associated with decreased whole-body insulin sensitivity and

unfavorable body composition and serum metabolomics. Cerebral ECS regulates food intake and energy balance by interacting with reward pathways and orexigenic and anorexigenic hormones. It seems that, during a sustained positive energy balance, the cerebral ECS may become dysregulated, accompanied by defective leptin and insulin signaling, resulting in peripheral WAT accumulation and increased EGP [4], whereas pharmacologic or genetic inhibition of CB1Rs results in reduced food intake and it has antiobesity effects [4, 5, 9].

In white adipocytes, CB1R activation has several effects promoting the development of obesity and insulin resistance. CB1R activation increases adipocyte differentiation and adipogenesis, enhances fatty acid synthesis and triglyceride accumulation, reduces lipolysis, and decreases mitochondrial biogenesis favoring white and inhibiting the brown and beige phenotype, thus participating in the regulation of thermogenesis and energy expenditure. CB1R inhibition has reverse actions [4, 7, 9]. So far, the role of adipose tissue ECS in human obesity has been investigated mainly by measuring circulating and tissue endocannabinoid levels and by studying the gene expression of CB1Rs and endocannabinoid degrading enzymes [27–31]. Higher levels of circulating endocannabinoids have been observed in patients with obesity as compared with lean patients and they have been shown to decrease after weight loss [27, 28, 32, 33]. Circulating 2-AG levels were found to correlate positively with fasting insulin and triglycerides and negatively with HDL cholesterol levels [29]. Higher 2-AG levels have also been measured in VAT [33, 34], but they have been shown to be reduced in abdominal SAT [31, 35] in obesity; thus it has been proposed that alterations in endocannabinoid levels might occur in a WAT-depot-specific manner [4]. Discrepancy exists concerning CB1R expression in obesity. In high-fat fed [36] and obese Zucker rats [37], adipocyte hypertrophy has been shown to associate with increased CB1R expression in adipose tissue, whereas in humans with obesity, increased endocannabinoid levels in VAT were observed simultaneously with a trend toward a decrease of CB1R levels in VAT [34]. Also, lower CB1R gene expression has been found in abdominal SAT and VAT in patients with obesity compared with lean patients [27, 28, 31], and weight loss was followed by an increase of CB1R gene expression in abdominal SAT [31]. The expression of endocannabinoid degrading enzymes has been found to be differently affected by obesity, adipose tissue depot, and weight loss [27, 28, 30, 31, 38].

Unlike studying gene expression rate from tissue biopsies, [^{18}F]FMPEP- d_2 PET does not reveal the total CB1R density in the tissue. Instead, [^{18}F]FMPEP- d_2 binds to CB1Rs that are not occupied with their ligands endocannabinoids. Therefore, the reduced binding of [^{18}F]FMPEP- d_2 in tissues or reduced CB1R availability in tissues of the HR participants we found can either reflect increased endocannabinoid levels and their binding to CB1Rs, decreased CB1R expression in the tissue, or reduced CB1R affinity. Tissue endocannabinoid levels were not assessed in our study. Circulating endocannabinoid levels did not differ between the study groups, although we observed correlations between endocannabinoid levels and BMI, insulin sensitivity, and serum lipid and GlycA levels consistent with previous findings [27, 29]. It is acknowledged that a positive energy balance results in ECS dysregulation and an increase in the peripheral endocannabinoid tone [4, 8, 34], but the mechanisms of action of the ECS are still not fully understood. The regulation of CB1R expression seems to be complex.

Insulin has a central role in endocannabinoid metabolism in WAT [34]. In cultured adipocytes, insulin reduces intracellular endocannabinoid levels, but it does not affect the expression of CB1Rs. In insulin-resistant adipocytes, the insulin action on the endocannabinoid tone is absent or reversed. Similar observations were made with insulin-

resistant obese mice [33]. It is thus possible that the negative correlations between endocannabinoid levels and whole-body insulin sensitivity and the positive correlations between WAT CB1R availability and GU rates we found would represent the relationship between insulin action, or insulin resistance, and ECS dysregulation in WAT. In addition to insulin, the endocannabinoid tone in WAT is under control of central leptin signaling [39]. As obesity is characterized by leptin resistance, a study with obese mice showed that a peripherally restricted CB1R inverse agonist reduced food intake, body weight, and adiposity by suppressing the secretion and increasing the clearance of leptin [40].


In skeletal muscle, CB1Rs are thought to participate in the glucose homeostasis by decreasing GU after CB1R activation. There are differing results whether the ECS tone in muscle becomes dysregulated under conditions of obesity [4, 8, 9]. In the present study, CB1R availability of skeletal muscle did not differ between the groups, nor did it correlate with insulin sensitivity, possibly because of the young and healthy state of the participants. Our study did not show differences in CB1R availability of BAT. In a previous study [11], the difference was observed under cold exposure: the increase in CB1R availability of BAT in cold was blunted in participants with obesity as compared with lean participants.

Interestingly, linoleic acid, a precursor for endocannabinoids, correlated positively with AG (1 + 2) level and negatively with CB1R availability of IWAT. Excessive intake of linoleic acid has been implicated in the development of obesity, in which one possible pathway is the formation of endocannabinoids [41]. In mice, a diet enriched with linoleic acid increased liver endocannabinoid and plasma leptin levels, food intake, body weight, and adiposity, whereas adding dietary omega-3 fatty acids along with linoleic acid reversed the actions [42]. Accordingly, we observed positive correlations with linoleic acid and body adiposity, weight, and BMI. However, also ω -3 fatty acid level correlated positively with AG (1 + 2) and negatively with CB1R availability of muscle, and we do not have a suggested explanation for this. To control the overactive ECS, promising results have been found in studies with diets enriched in omega-3 fatty acids: reduced peripheral endocannabinoid levels, reduced waist to hip and visceral fat/skeletal muscle mass ratios, and improved lipid profile in participants with obesity [43].

This study had some limitations. We found lower [^{18}F]FMPEP- d_2 binding in abdominal adipose tissue in HR as compared with LR participants. However, the PET measurement is not able to distinguish a change in total CB1R density or affinity or whether CB1R availability is a consequence of a change in tissue or circulating endocannabinoid levels. We only studied males. The ECS interacts with gonadal hormones; central endocannabinoid signaling primarily reduces the release of gonadal hormones, whereas gonadal hormones cause changes in protein expression in ECS [44]. Estrogen negatively modulates ECS-induced changes in appetite, body temperature, and hypothalamic proopiomelanocortin (POMC) neurons [45]. It is thus not certain whether our result can be generalized to females. Because endocannabinoids are produced and released on demand, it is not possible to distinguish the source of the measured compounds. However, the similar associations with previously published studies with

circulating endocannabinoids and different variables we found encourage us to believe that the measured endocannabinoids do represent a metabolic situation of the body. Finally, the cross-sectional nature of the study precludes causal inference regarding the observed associations.

CONCLUSION

Here we have demonstrated lower CB1R availability of abdominal adipose tissue in young healthy patients with overweight and risk for obesity as compared with lean patients with no obesity risk and associations between CB1R availability of abdominal adipose tissue and the whole brain and insulin sensitivity and serum metabolomics. Our results suggest altered endocannabinoid tone in abdominal adipose tissue of participants with overweight, possibly reflecting a broader dysregulation of ECS with energy imbalance. 

AUTHOR CONTRIBUTIONS

Laura Pekkarinen: study design, coordination, data acquisition, modeling, statistical analysis, interpretation of results, tables and figures, main writer of the manuscript. Tatu Kantonen: study design, coordination, data acquisition, modeling, statistical analysis, interpretation of results. Vesa Oikonen: [^{18}F]FMPEP- d_2 data modeling. Merja Haaparanta-Solin, Richard Aarnio: analysis of [^{18}F]FMPEP- d_2 metabolites. Alex M. Dickens, Annie von Eyken: endocannabinoid measurements. Aino Latva-Rasku: participation in FDG PET data analysis. Prince Dadson: analysis of tissue masses. Anna K. Kirjavainen, Johan Rajander: radiotracer production. Kari Kalliokoski, Tapani Rönnemaa: study design. Lauri Nummenmaa: study design, coordination, statistical analysis, interpretation of results, figures, manuscript editing, study supervision. Pirjo Nuutila: study design, coordination, interpretation of results, study supervision. All authors were involved in writing the paper and had final approval of the submitted and published versions.

ACKNOWLEDGMENTS

The authors thank the volunteers who participated in this study and the staff of the Turku PET Centre.

FUNDING INFORMATION

The study was supported by Center of Excellence funding #307402 to Pirjo Nuutila, Academy of Finland grants #294897 and #332225 to Lauri Nummenmaa, Turku University Hospital Foundation for Education and Research, The Diabetes Research Foundation and Orion Research Foundation to Laura Pekkarinen, Finnish Cultural Foundation (Southwest Finland Fund), Emil Aaltonen Foundation, and Jenny and Antti Wihuri Foundation to Tatu Kantonen.

CONFLICT OF INTEREST STATEMENT

The authors declared no conflict of interest.

ORCID

Laura Pekkarinen  <https://orcid.org/0000-0002-5596-0485>

Pirjo Nuutila  <https://orcid.org/0000-0001-9597-338X>

REFERENCES

- World Health Organization. World Obesity Day 2022 – Accelerating action to stop obesity. Published March 4, 2022. <https://www.who.int/news/item/04-03-2022-world-obesity-day-2022-accelerating-action-to-stop-obesity>
- Pi-Sunyer FX. The obesity epidemic: pathophysiology and consequences of obesity. *Obes Res*. 2002;10(suppl 2):97S-104S. doi:10.1038/oby.2002.202
- Bermudez-Silva FJ, Viveros MP, McPartland JM, Rodriguez de Fonseca F. The endocannabinoid system, eating behavior and energy homeostasis: the end or a new beginning? *Pharmacol Biochem Behav*. 2010;95(4):375-382.
- Silvestri C, Di Marzo V. The endocannabinoid system in energy homeostasis and the etiopathology of metabolic disorders. *Cell Metab*. 2013;17(4):475-490.
- Di Marzo V, Matias I. Endocannabinoid control of food intake and energy balance. *Nat Neurosci*. 2005;8(5):585-589.
- Gatta-Cherifi B, Cota D. New insights on the role of the endocannabinoid system in the regulation of energy balance. *Int J Obes*. 2016;40(2):210-219. doi:10.1038/ijo.2015.179
- Quarta C, Mazza R, Obici S, Pasquali R, Pagotto U. Energy balance regulation by endocannabinoids at central and peripheral levels. *Trends Mol Med*. 2011;17(9):518-526.
- Di Marzo V. The endocannabinoid system in obesity and type 2 diabetes. *Diabetologia*. 2008;51(8):1356-1367.
- Simon V, Cota D. Mechanisms in endocrinology: endocannabinoids and metabolism: past, present and future. *Eur J Endocrinol*. 2017;176(6):R309-R324.
- Kantonen T, Pekkarinen L, Karjalainen T, et al. Obesity risk is associated with altered cerebral glucose metabolism and decreased μ -opioid and CB1 receptor availability. *Int J Obes*. 2022;46(2):400-407.
- Lahtesmaa M, Eriksson O, Gnad T, et al. Cannabinoid type 1 receptors are upregulated during acute activation of brown adipose tissue. *Diabetes*. 2018;67(7):1226-1236.
- Juonala M, Juhola J, Magnussen CG, et al. Childhood environmental and genetic predictors of adulthood obesity: the cardiovascular risk in young Finns study. *J Clin Endocrinol Metab*. 2011;96(9):E1542-E1549.
- Juhola J, Magnussen CG, Viikari JSA, et al. Tracking of serum lipid levels, blood pressure, and body mass index from childhood to adulthood: the cardiovascular risk in young Finns study. *J Pediatr*. 2011;159(4):584-590.
- Endalifer ML, Diress G. Epidemiology, predisposing factors, biomarkers, and prevention mechanism of obesity: a systematic review. *J Obes*. 2020;2020:6134362. doi:10.1155/2020/6134362
- Mattsson N, Rönnemaa T, Juonala M, Viikari JSA, Raitakari OT. Childhood predictors of the metabolic syndrome in adulthood. The cardiovascular risk in young Finns study. *Ann Med*. 2008;40(7):542-552.
- Cederberg H, Stančáková A, Kuusisto J, Laakso M, Smith U. Family history of type 2 diabetes increases the risk of both obesity and its complications: is type 2 diabetes a disease of inappropriate lipid storage? *J Intern Med*. 2015;277(5):540-551. doi:10.1111/joim.12289
- Anjana RM, Lakshminarayanan S, Deepa M, Farooq S, Pradeepa R, Mohan V. Parental history of type 2 diabetes mellitus, metabolic syndrome, and cardiometabolic risk factors in Asian Indian adolescents. *Metabolism*. 2009;58(3):344-350.

18. Karlsson HK, Tuominen L, Tuulari JJ, et al. Obesity is associated with decreased μ -opioid but unaltered dopamine D2 receptor availability in the brain. *J Neurosci*. 2015;35(9):3959-3965.
19. Lahdenpohja S, Keller T, Forsback S, et al. Automated GMP production and long-term experience in radiosynthesis of CB(1) tracer [(18) F]FMPEP-d(2). *J Labelled Comp Radiopharm*. 2020;63(9):408-418.
20. Hamacher K, Coenen HH, Stöcklin G. Efficient stereospecific synthesis of no-carrier-added 2-[18F]-fluoro-2-deoxy-D-glucose using aminopolyether supported nucleophilic substitution. *J Nucl Med*. 1986;27(2):235-238.
21. Lemaire C, Damhaut P, Lauricella B, et al. Fast F-18 FDG synthesis by alkaline hydrolysis on a low polarity solid phase supports. *Labelled Comp Radiopharm*. 2002;45(5):435-447.
22. Din M U, Raiko J, Saari T, et al. Human brown fat radiodensity indicates underlying tissue composition and systemic metabolic health. *J Clin Endocrinol Metab*. 2017;102(7):2258-2267.
23. Eriksson O, Mikkola K, Espes D, et al. The cannabinoid receptor-1 is an imaging biomarker of brown adipose tissue. *J Nucl Med*. 2015;56(12):1937-1941.
24. DeFronzo RA, Tobin JD, Andres R. Glucose clamp technique: a method for quantifying insulin secretion and resistance. *Am J Physiol*. 1979;237(3):E214-E223.
25. Soininen P, Kangas AJ, Würtz P, Suna T, Ala-Korpela M. Quantitative serum nuclear magnetic resonance metabolomics in cardiovascular epidemiology and genetics. *Circ Cardiovasc Genet*. 2015;8(1):192-206.
26. Dickens AM, Borgan F, Laurikainen H, et al. Links between central CB1-receptor availability and peripheral endocannabinoids in patients with first episode psychosis. *NPJ Schizophr*. 2020;6(1):21. doi:10.1038/s41537-020-00110-7
27. Blüher M, Engeli S, Klötting N, et al. Dysregulation of the peripheral and adipose tissue endocannabinoid system in human abdominal obesity. *Diabetes*. 2006;55(11):3053-3060.
28. Engeli S, Böhnke J, Feldpausch M, et al. Activation of the peripheral endocannabinoid system in human obesity. *Diabetes*. 2005;54(10):2838-2843.
29. Côté M, Matias I, Lemieux I, Petrosino S, et al. Circulating endocannabinoid levels, abdominal adiposity and related cardiometabolic risk factors in obese men. *Int J Obes*. 2007;31(4):692-699.
30. Sarzani R, Bordinchia M, Marcucci P, et al. Altered pattern of cannabinoid type 1 receptor expression in adipose tissue of dysmetabolic and overweight patients. *Metabolism*. 2009;58(3):361-367.
31. Bennetzen MF, Wellner N, Ahmed SS, et al. Investigations of the human endocannabinoid system in two subcutaneous adipose tissue depots in lean subjects and in obese subjects before and after weight loss. *Int J Obes*. 2011;35(11):1377-1384.
32. Di Marzo V, Côté M, Matias I, et al. Changes in plasma endocannabinoid levels in viscerally obese men following a 1 year lifestyle modification programme and waist circumference reduction: associations with changes in metabolic risk factors. *Diabetologia*. 2009;52(2):213-217.
33. D'Eon TM, Pierce KA, Roix JJ, Tyler A, Chen H, Teixeira SR. The role of adipocyte insulin resistance in the pathogenesis of obesity-related elevations in endocannabinoids. *Diabetes*. 2008;57(5):1262-1268.
34. Matias I, Gonthier MP, Orlando P, et al. Regulation, function, and dysregulation of endocannabinoids in models of adipose and beta-pancreatic cells and in obesity and hyperglycemia. *J Clin Endocrinol Metab*. 2006;91(8):3171-3180.
35. Izzo AA, Piscitelli F, Capasso R, et al. Peripheral endocannabinoid dysregulation in obesity: relation to intestinal motility and energy processing induced by food deprivation and re-feeding. *Br J Pharmacol*. 2009;158(2):451-461.
36. Yan ZC, Liu DY, Zhang LL, et al. Exercise reduces adipose tissue via cannabinoid receptor type 1 which is regulated by peroxisome proliferator-activated receptor-delta. *Biochem Biophys Res Commun*. 2007;354(2):427-433.
37. Bensaid M, Gary-Bobo M, Esclangon A, et al. The cannabinoid CB1 receptor antagonist SR141716 increases Acpr30 mRNA expression in adipose tissue of obese fa/fa rats and in cultured adipocyte cells. *Mol Pharmacol*. 2003;63(4):908-914.
38. Bordinchia M, Battistoni I, Mancinelli L, et al. Cannabinoid CB1 receptor expression in relation to visceral adipose depots, endocannabinoid levels, microvascular damage, and the presence of the Cnr1 A3813G variant in humans. *Metabolism*. 2010;59(5):734-741.
39. Buettner C, Muse ED, Cheng A, et al. Leptin controls adipose tissue lipogenesis via central, STAT3-independent mechanisms. *Nat Med*. 2008;14(6):667-675.
40. Tam J, Cinar R, Liu J, et al. Peripheral cannabinoid-1 receptor inverse agonism reduces obesity by reversing leptin resistance. *Cell Metab*. 2012;16(2):167-179.
41. Naughton SS, Mathai ML, Hryciw DH, McAinch AJ. Linoleic acid and the pathogenesis of obesity. *Prostaglandins Other Lipid Mediat*. 2016;125:90-99.
42. Alveheim AR, Malde MK, Osei-Hyiaman D, et al. Dietary linoleic acid elevates endogenous 2-AG and anandamide and induces obesity. *Obesity*. 2012;20(10):1984-1994.
43. Berge K, Piscitelli F, Hoem N, et al. Chronic treatment with krill powder reduces plasma triglyceride and anandamide levels in mildly obese men. *Lipids Health Dis*. 2013;12:78. doi:10.1186/1476-511X-12-78
44. Gorzalka BB, Dang SS. Minireview: endocannabinoids and gonadal hormones: bidirectional interactions in physiology and behavior. *Endocrinology*. 2012;153(3):1016-1024.
45. Kellert BA, Nguyen MC, Nguyen C, Nguyen QH, Wagner EJ. Estrogen rapidly attenuates cannabinoid-induced changes in energy homeostasis. *Eur J Pharmacol*. 2009;622(1-3):15-24.

SUPPORTING INFORMATION

Additional supporting information can be found online in the Supporting Information section at the end of this article.

How to cite this article: Pekkarinen L, Kantonen T, Oikonen V, et al. Lower abdominal adipose tissue cannabinoid type 1 receptor availability in young men with overweight. *Obesity (Silver Spring)*. 2023;31(7):1844-1858. doi:10.1002/oby.23770